ARMY RESEARCH LABORATORY

Spall Strength of Silicon Carbide Under Normal and Simultaneous Compression-Shear Shock Wave Loading

by Dattatraya P. Dandekar

ARL-RP-83 **September 2004**

A reprint from the *International Journal of Applied Ceramics Technology*, vol. 1, no. 3, pp. 261–268, 2004.

Approved for public release; distribution is unlimited.

NOTICES

Disclaimers

The findings in this report are not to be construed as an official Department of the Army position unless so designated by other authorized documents.

Citation of manufacturer's or trade names does not constitute an official endorsement or approval of the use thereof.

Destroy this report when it is no longer needed. Do not return it to the originator.

Army Research Laboratory
Aberdeen Proving Ground, MD 21005-5066

ARL-RP-83 **September 2004**

Spall Strength of Silicon Carbide Under Normal and Simultaneous Compression-Shear Shock Wave Loading

Dattatraya P. Dandekar
Weapons and Materials Research Directorate, ARL

A reprint from the *International Journal of Applied Ceramics Technology*, vol. 1, no. 3, pp. 261–268, 2004.

Approved for public release; distribution is unlimited.

REPORT DOCUMENTATION PAGE

Form Approved
OMB No. 0704-0188

Public reporting burden for this collection of information is estimated to average 1 hour per response, including the time for reviewing instructions, searching existing data sources, gathering and maintaining the data needed, and completing and reviewing the collection information. Send comments regarding this burden estimate or any other aspect of this collection of information, including suggestions for reducing the burden, to Department of Defense, Washington Headquarters Services, Directorate for Information Operations and Reports (0704-0188), 1215 Jefferson Davis Highway, Suite 1204, Arlington, VA 22202-4302. Respondents should be aware that notwithstanding any other provision of law, no person shall be subject to any penalty for failing to comply with a collection of information if it does not display a currently valid OMB control number.
PLEASE DO NOT RETURN YOUR FORM TO THE ABOVE ADDRESS.

1. REPORT DATE *(DD-MM-YYYY)*	2. REPORT TYPE	3. DATES COVERED (From - To)
September 2004	Reprint	July 2003–October 2004

4. TITLE AND SUBTITLE
Spall Strength of Silicon Carbide Under Normal and Simultaneous Compression-Shear Shock Wave Loading

5a. CONTRACT NUMBER

5b. GRANT NUMBER

5c. PROGRAM ELEMENT NUMBER

6. AUTHOR(S)
Dattatraya P. Dandekar

5d. PROJECT NUMBER
AH43

5e. TASK NUMBER

5f. WORK UNIT NUMBER

7. PERFORMING ORGANIZATION NAME(S) AND ADDRESS(ES)
U.S. Army Research Laboratory
ATTN: AMSRD-ARL-WM-TD
Aberdeen Proving Ground, MD 21005-5066

8. PERFORMING ORGANIZATION REPORT NUMBER
ARL-RP-83

9. SPONSORING/MONITORING AGENCY NAME(S) AND ADDRESS(ES)

10. SPONSOR/MONITOR'S ACRONYM(S)

11. SPONSOR/MONITOR'S REPORT NUMBER(S)

12. DISTRIBUTION/AVAILABILITY STATEMENT
Approved for public release; distribution is unlimited.

13. SUPPLEMENTARY NOTES
*A reprint from the *International Journal of Applied Ceramics Technology*, vol. 1, no. 3, pp. 261–268, 2004.

14. ABSTRACT
Spall strength data of sintered and hot-pressed silicon carbide show an initial increase with an increase in the shock-induced stress to around 4 GPa. At impact stress around 6 GPa and above, spall strength data of these materials show a continuous decrease in the magnitude of spall strength. This unusual trend in the spall strength of silicon carbides may be due to the competing roles of (i) localized plasticity, (ii) generation and propagation of cracks taking into consideration their relative dominance below and above a given magnitude of stress. This work presents the results of spall experiments conducted to test the relative dominance hypothesis by determining whether the observed initial increase in spall strength of silicon carbide is due to dominance of localized plastic deformation over crack-dominated brittle deformation, while the observed decline in the spall strength with an increase in the shock-induced stress reflects a dominance of crack-induced brittle deformation over plastic deformation.

15. SUBJECT TERMS
spall, silicon carbide, shock, failure front

16. SECURITY CLASSIFICATION OF:			17. LIMITATION OF ABSTRACT	18. NUMBER OF PAGES	19a. NAME OF RESPONSIBLE PERSON
					Dattatraya P. Dandekar
a. REPORT	b. ABSTRACT	c. THIS PAGE			19b. TELEPHONE NUMBER (*Include area code*)
UNCLASSIFIED	UNCLASSIFIED	UNCLASSIFIED	UL	18	(410) 306-0779

Standard Form 298 (Rev. 8/98)
Prescribed by ANSI Std. Z39.18

International Journal of
Applied Ceramic Technology
Ceramic Product Development and Commercialization

Spall Strength of Silicon Carbide Under Normal and Simultaneous Compression-Shear Shock Wave Loading

Dattatraya P. Dandekar

U.S. Army Research Laboratory, Aberdeen Proving Ground, MD 21005-5069

Spall strength data of sintered and hot-pressed silicon carbide show an initial increase with an increase in the shock-induced stress to around 4 GPa. At impact stress around 6 GPa and above, spall strength data of these materials show a continuous decrease in the magnitude of spall strength.[1] This unusual trend in the spall strength of silicon carbides may be due to the competing roles of (i) localized plasticity, (ii) generation and propagation of cracks taking into consideration their relative dominance below and above a given magnitude of stress. This work presents the results of spall experiments conducted to test the relative dominance hypothesis by determining whether the observed initial increase in spall strength of silicon carbide is due to dominance of localized plastic deformation over crack-dominated brittle deformation, while the observed decline in the spall strength with an increase in the shock-induced stress reflects a dominance of crack-induced brittle deformation over plastic deformation.

Introduction

Accumulated experimental results pertaining to plane shock wave response of polycrystalline ceramics indicate that while their compressive and shear strengths tend to be very high their tensile strengths are extremely low. The compressive and shear strengths of these materials do not degrade significantly even in the presence of moderate pore volume fraction (less than 1-2%) or a small population of micro-cracks/fissures. Their tensile strengths degrade significantly in the presence of pore volume fraction, and cracks/fissures (micro and/or meso). Ewart and Dandekar[2] showed that degradation of tensile strength, i.e., spall strength of titanium diboride, could be linked to an increase in the population and average lengths of micro-cracks.

However, in terms of experimental data, dependence on the pore volume fraction is less clear. Since pores are potential sites for generation of micro-cracks/fissures in the ceramics under shock compression and also possibly under release of shock compression, the effect of pores cannot be isolated completely from those of micro-cracks/fissures.

Bartkowski and Dandekar[1] reported an initial increase in the spall strength of sintered and hot-pressed silicon carbide (SiC-B) with an increase in the magnitude of shock-wave-induced stress to 3.8 GPa. Onset of a decline in the spall strength was observed to begin in these silicon carbides when shocked beyond 5.8 GPa. Dandekar and Bartkowski[3,4] later reported that this same unusual trend in spall strength was also observed in sintered and subsequently hot-pressed silicon carbides produced in France, with one significant difference: Whereas the sintered silicon carbide mimicked the trend observed in [1], the spall strength of French sintered and subsequently hot-pressed continued to increase to 12 GPa before showing a decline in the spall strength with an increase in the shock-induced stress. A large scatter in the spall strength

of silicon carbide produced by Cercom Inc. and marketed as SiC-N displayed no clear trend with increasing magnitude of shock-induced stress.

The present investigation tests the hypothesis that a shifting dominance pattern can explain the observed trend in spall strength of silicon carbide, specifically SiC-B. According to the hypothesis, the observed initial increase in spall strength of silicon carbide is due to dominance of localized plastic deformation over the crack-dominated brittle deformation. The observed decline in the spall strength with an increase in the shock-induced stress is due to dominance of crack-induced brittle deformation over the plastic deformation. The observed initial increase in the spall strength of SiC-B suggests the envisaged dominance of localized plastic deformation over the crack-dominated brittle deformation continues to shock-induced stress of 3.8 GPa. The observed decline in the spall strength at 5.8 GPa designates that point as the stress at which dominance of crack-induced brittle deformation over the plastic deformation begins in SiC-B.

The validity of the suggested hypothesis is tested by measuring the spall strength of SiC-B at shock-induced stresses of 3.8 and 5.8 GPa (i) under normal impact without inducing a shear, and (ii) under oblique impact, i.e., under simultaneous compression shear. If the suggested hypothesis is valid then the spall strength of SiC-B will be either constant or increase at 3.8 GPa when localized plasticity dominates the inelastic deformation. The plastic deformation will be promoted under enhanced shock-induced shear, i.e., simultaneous compression shear compared to value under normal shock. On the other hand, at 5.8 Gpa, when deformation is dominantly controlled through cracks, the spall strength of SiC-B will be less under simultaneous compression shear than under normal shock.

Material

Silicon carbide, marketed as SiC-B by Cercom Inc., was produced by hot-pressing SiC-B powder. The processing of silicon carbide being proprietary, details of processing is not disclosed by the manufacturers. Mechanical properties of silicon carbide are found to be dependent on (i) grain size of the powder, (ii) processing temperature, (iii) sintering aids, (iv) powder blending process, and (v) elemental composition and stoichiometry of the compounds present in the processed materials. All powders have some metallic impurities introduced during the powder manufacturing process. In addition, silicon carbide cannot be consolidated without sintering aids. The conventional sintering aids for consolidation of silicon carbide powder are boron, carbon, and aluminum nitride. Aluminum nitride is used as a sintering aid in producing SiC-B material. All impurities segregate in small, well-dispersed clusters along the SiC-B grain boundaries. The blended powder, containing silicon carbide and sintering aid, is loaded into a graphite die and then hot-pressed at around 2273 K under 18 MPa. Since 2273 K is higher than the melting temperature of the metallic impurities, the melted metals aggregate to form inclusions in the consolidated SiC-B. Sintering aids promote formation of these inclusions by creating favorable environs to wet silicon carbide grain surfaces, thus spreading the melt. The average grain size of this material is 4 μm with the size ranging between 2-10 μm. The density of the material is 3.215 ± 0.002 Mg/m^3. The measured values of longitudinal and shear wave velocities in SiC-B are 12.198 ± 0.026 and 7.747 ± 0.018 km/s, respectively[1,3,4].

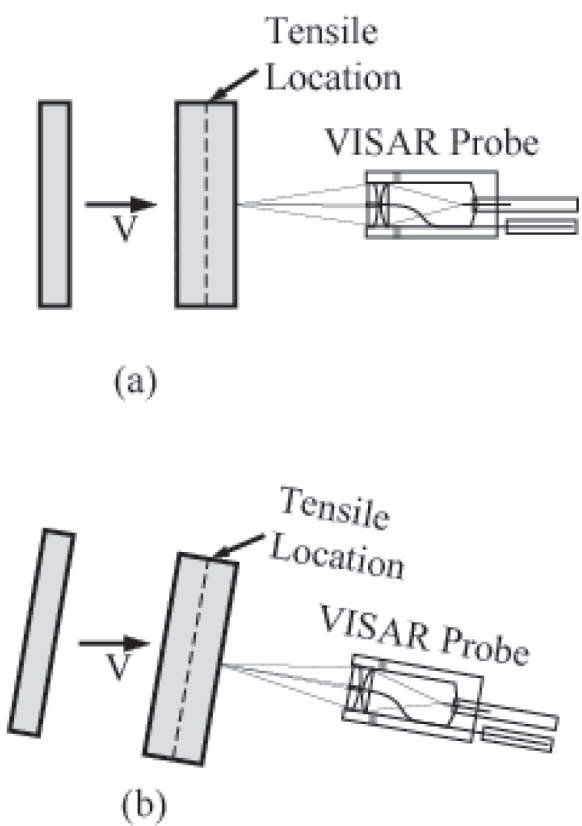

Fig. 1. Experiment configurations: (a) normal, and (b) compression shear.

The values of Young's, shear, and bulk moduli are 448 ± 2, 193 ± 1, and 221 ± 2 GPa, respectively. The Poisson's ratio is 0.162 ± 0.003.

Experiment

A general configuration of normal and simultaneous compression shear spall experiments performed on SiC is shown in Fig. 1. The experiment consists of impacting a stationary disc (target) of SiC with another disc (flyer) of SiC, at a given impact velocity (V). Flyers are thinner than the targets in spall experiments. The impact may be normal as shown in Fig. 1(a) or at some obliquity to induce simultaneous compression and shear as shown in Fig. 1(b). The free surface velocity profile of the target is monitored to provide information about the initial shock compression and the following release and tension developed in the target. The velocity profiles were recorded by means of a Velocity Interferometer System for Any Reflecting surface (VISAR) developed by Barker and Hollenbach.[5]

Rectangular specimens of SiC-B used in the shock wave experiments had a lateral dimension of 50 ± 0.5 mm. The thicknesses of the SiC-B specimens used are given in Table I. SiC-B disc faces were lapped and polished flat to 5 µm. The opposing disc faces were mutually parallel to within one part in 10^4. The SiC-B specimen surface was polished to reflect the VISAR beam.

Impact velocity of the flyer disc is recorded by means of shorting four sets of electrically charged pins located immediately in front of the target. Pin distances are premeasured. Time between pins is measured during the experiment so that velocity of impact can be calculated. The precision of impact velocity measurements is generally within 0.5%. Impact tilt is less than 0.5 mrad. The precision of particle velocity measurements using the VISAR is 1%. Further details of this type of experiments are given in [1].

Results

Ten experiments were performed on SiC-B. Table I summarizes the details of these experiments. The results of spall experiments are summarized in Table II. Table I shows that the recorded free surface velocity labeled as shock and recompression are identical to the normal component of the impact velocity. A similar comment holds for the measured and calculated pulse widths. This is not surprising since the shock stresses of 3.9 ± 0.1 and 5.8 ± 0.1 GPa are less than the HEL of SiC-B, i.e., 12-15 GPa. A primary advantage of these observations is that induced shear stress given in Table II could be confidently calculated using the elastic theory. The other significant results of this work are presented separately for each of the two shock-induced stresses, i.e., 3.9 ± 0.1 and 5.8 ± 0.1 GPa.

Results of Spall Experiments at 3.9 ± 0.1 GPa

Free surface velocity profiles recorded in experiments

Table I. Data from Shock Wave Experiments in SiC-B

Experiment	Impactor Thickness (mm)	Target Thickness (mm)	Obliquity Degrees	Impact Actual (Km/s)	velocity Normal component	Pulse Measured (µs)	width Calculated (µs)	Free Shock (Km/s)	surface Spall (Km/s)	velocity Recompression (Km/s)
0206	5.149	7.719	0	0.204	0.204	0.82	0.84	0.203	0.169	0.203
0207	5.156	7.721	0	0.304	0.304	0.82	0.84	0.309	0.298	0.309
0208	5.148	7.705	12	0.206	0.201	0.85	0.84	0.200	0.160	0.200
0209#	5.145	7.723	12	0.297	0.290	-		0.291	none	0.318
0210	5.14	7.74	0	0.207	0.207	0.84	0.84	0.205	0.170	0.205
0211	3.88	7.712	0	0.197	0.197	0.64	0.64	0.203	0.166	0.203
0212#	5.142	7.718	12	0.306	0.299			0.297	none	0.309
0305	1.353	6.410	12	0.303	0.296	0.248	0.222	0.300	0.280	0.300
0307#	6.425	5.125	12	0.296	0.289			0.295	none	0.306
0314	1.343	6.421	20	0.204	0.192	0.238	0.220	0.189	0.126	0.189

#In these experiments, spall related pull-back velocities were not observed due to propagation of a failure front in SiC-B. The recompression values are those related to the re-acceleration of free surface velocity due to the failure front propagation (see text).

Table II. Summary of the Results of Shock Wave Experiments in SiC-B

Experiment	Obliquity Degrees	Impact velocity Actual (km/s)	Impact velocity Normal component (km/s)	Impact velocity Tangential component (km/s)	Shock-induced stress Longitudinal (GPa)	Shock-induced stress Shear (GPa)	Spall 1/2 Pull-back velocity (km/s)	Spall Strength (GPa)
0206	0	0.204	0.204	None	4.00	None	0.017	0.67
0207	0	0.304	0.304	None	5.96	None	0.006	0.24
0208	12	0.206	0.201	0.043	3.94	0.54	0.020	0.78
0209#	12	0.297	0.290	0.062	5.69	0.77	None	None
0210	0	0.208	0.208	None	4.08	None	0.018	0.70
0211	0	0.197	0.197	None	3.86	None	0.0185	0.72
0212#	12	0.306	0.299	0.064	5.86	0.80	None	None
0305	12	0.303	0.296	0.063	5.80	0.78	0.010	0.39
0307#	12	0.296	0.289	0.062	5.67	0.77	None	None
0314	20	0.204	0.192	0.070	3.76	0.87	0.0315	1.23

#In these experiments, spall related pull-back velocities were not observed due to propagation of a failure front in SiC-B. The recompression values are those related to the re-acceleration of free surface velocity due to the failure front propagation (see text).

at 3.9 ± 0.1 GPa on SiC-B are shown in Fig. 2. The values of spall strength obtained from experiments 0206 and 0210 at normal impact are 0.67 ± 0.03 and 0.70 ± 0.03 GPa, respectively. These values are significantly smaller than the magnitude of spall strength found earlier[1] for this material, i.e., 1.3 GPa. The SiC-B materials used in both studies were fabricated by Cercom Inc, but came from batches manufactured a few years apart. Further, the compressive shock durations (pulse widths) in the present work and the previous work are 0.82 and 0.64 µs, respectively. In order to investigate whether or not the observed large difference in the values of spall strength at 3.9 GPa may be due to the difference in compressive durations of the shock, experiment 0211 was performed. Compressive duration in this experiment was 0.64 µs. Free surface velocity profiles recorded in experiment 0211 and [1] shown in Fig. 3 show the difference in the spall generated signals in SiC-B from different batches for a

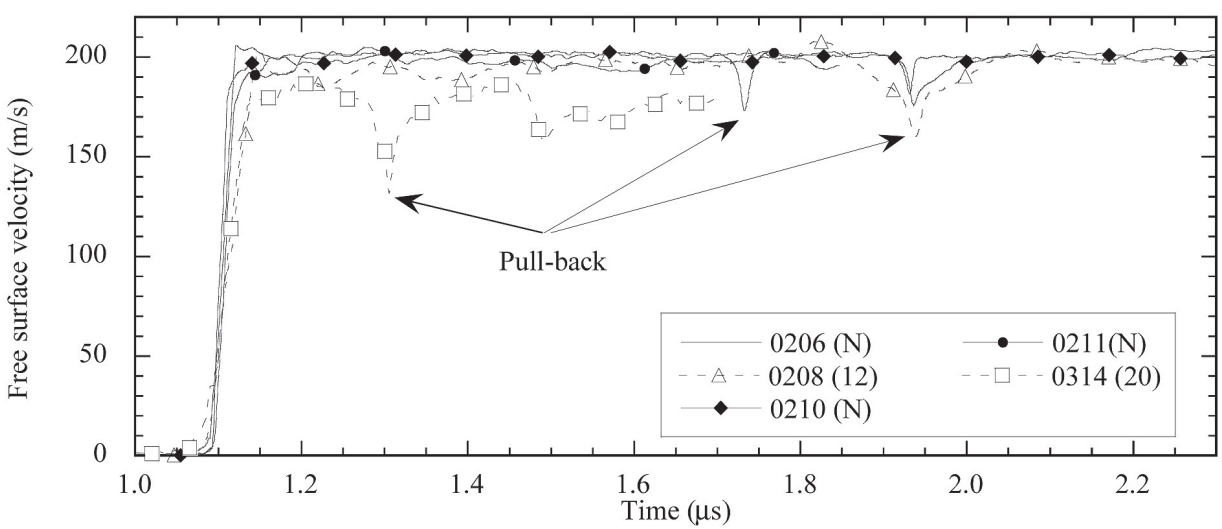

Fig. 2. Free surface velocity profiles recorded in experiments at 3.9 ± 0.1 GPa on SiC-B. In this figure N and 12 in parentheses indicate obliquity of 0° and 12° impact.

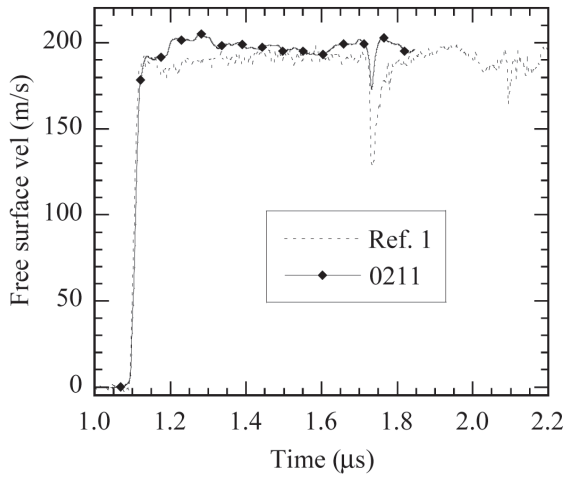

Fig. 3. Free surface velocity profiles from experiment 0211 and [1] at 3.9 GPa under normal impact.

pulse width of 0.64 μs. The value of spall strength obtained in experiment 0211 is 0.70 ± 0.03 GPa, a value close to those in experiments 0206 and 0210. This is consistent with the results of spall strength of SiC-B in the previous work,[4] namely, the spall strength of SiC-B was not found to be sensitive to the compressive shock duration. Thus the observed difference in the spall strength of SiC-B measured in the present work and the previous work is suspected to be due to batch-to-batch variation.

Experiments 0208 and 0314 were conducted at 12° and 20° of obliquity to subject SiC-B to simultaneous compression and shear. In these two experiments, SiC-B was subjected to a longitudinal shock of magnitudes 3.94 and 3.76 GPa and associated shear stresses of magnitudes 0.54 and 0.87 GPa, respectively. The magnitudes of spall strengths of SiC-B increase moderately to 0.78 ± 0.04 GPa at 12° obliquity, and upon an additional increase of obliquity to 20°, the spall strength assumes a value of 1.23 ± 0.06 GPa. This magnitude of spall strength is 75% more than determined under normal impact. These results are consistent with the hypothesis that the observed initial increase in spall strength of SiC-B to 3.9 GPa is due to dominance of localized plastic deformation over the crack-dominated brittle deformation in SiC-B.

Results of Experiments at 5.8 ± 0.1 GPa

Due to the observed batch-to-batch variation in the spall strength of SiC-B at 3.9 GPa, experiment 0207 was conducted to determine the spall strength of SiC-B under normal impact to facilitate an unambiguous comparison of spall strength of SiC-B determined from simultaneous compression shear at shock-induced stress of 5.8 ± 0.1 GPa. The free surface velocity profile recorded in this experiment is shown in Fig. 4. The ordinate is truncated to show the range of free surface velocity between 160 and 340 m/s to show the small value of spall with clarity. The result of experiment 0207 yielded a spall strength of

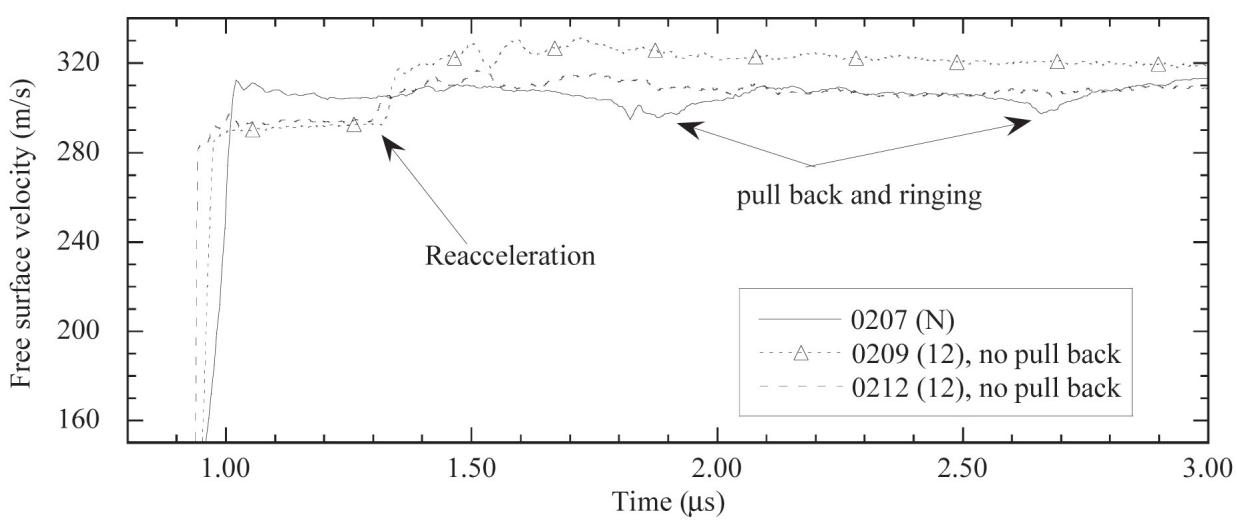

Fig. 4. Free surface velocity profiles recorded in experiments at 5.8 ± 0.1 GPa on SiC-B under normal impact and under simultaneous compression and shear.

0.24 ± 0.06 GPa for the batch of SiC-B used in the present work. Once again, this spall strength value, significantly smaller than the value of 1.1 GPa determined by Bartkowski and Dandekar,[1] is consistent with the smaller spall strength values obtained for SiC-B used in the present investigation at 3.9 GPa.

Fig. 4 also shows the free surface velocity profiles recorded in experiments 0209 and 0212. These two experiments were performed at 12° obliquity to measure spall strength of SiC-B under simultaneous compression shear. The values of longitudinal and shear stress induced in these experiments varied between 5.7-5.9 and 0.77-0.80 GPa, respectively (Table II). The free surface velocity profiles do not show the pull back due to spallation as in experiment 0207. Instead, the free surface velocity profiles obtained in these experiments show a step increase reminiscent of free surface velocity profiles observed by Kanel, *et al.*,[6] in K8 Glass and by Dandekar and Beaulieu[7] in soda lime glass. The step increase in the free surface velocity profiles exceeds the value of impact velocity suggesting interaction of a release wave propagating in SiC-B from the free surface towards the impact surface with a slow-moving propagating failure front in SiC-B away from the impact surface. An additional experiment, 0307, was performed to obtain the free surface velocity profile in which the impacting specimen of SiC-B was thicker than the specimen of SiC-B in the target, but the target thickness was less than in experiments 0209 and 0212. Throughout experiment 0307 the SiC-B target remained under compressive stress. The free surface velocity profiles in these three experiments are shown in terms of time duration normalized with respect to the respective thickness of the SiC-B targets (Fig. 5). These three profiles show that the occurrence of re-acceleration of the free surface velocity in SiC-B scales with the thickness. In other words, the failure front travels with a constant velocity in SiC-B when shocked to 5.8 GPa under simultaneous compression shear at 12° of obliquity.

The failure front velocity is 6.5 ± 0.2 km/s, as calculated from the wave profiles shown in Fig. 5. The measured ultrasonic shear wave velocity in SiC-B is 7.747 ± 0.018 km/s. This large difference in the velocities precludes any possibility that the observed re-acceleration of free surface velocities in experiments 0209, 0212, and 0307 by normal velocity probes used in these experiments are somehow picking up a contribution induced by the shear wave velocity. It is also ruled out by the close agreement between the normal component of impact velocity with the measured free surface velocity due to shock (Table I). Brar and Bless[8] show that spall strength is negligible when the spall occurs in the region traversed by the failure front in soda lime glass. The magnitude of failure front velocity in SiC-B implies that the spall planes in the experiments 0209 and 0212 were 2.6 mm from the impact surface of the SiC-B targets while the failure front traveled into the SiC-B target to a distance of 5.3 mm from the impact surface before tension was generated in it. Thus, the absence of pull-back velocity in the free sur-

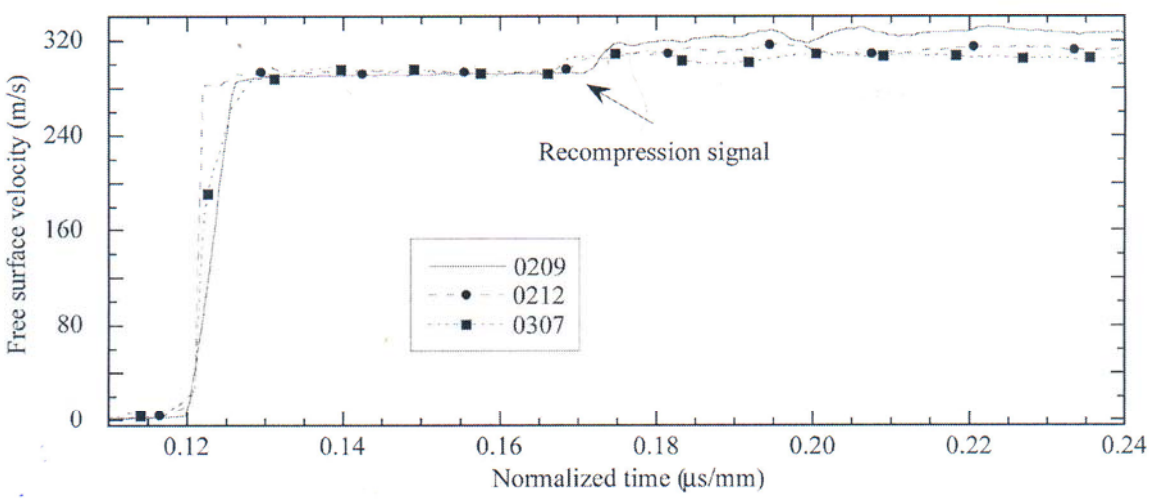

Fig. 5. Free surface velocity profiles in SiC-B targets at 5.8 ± 0.1 GPa under simultaneous compression and shear at 12° obliquity.

face velocity profiles in these two experiments could be due to a loss of spall strength of SiC-B in the failed region. Experiment 0305 was performed to determine whether the observed loss of spall strength of SiC-B was indeed due to the location of the spall plane in experiments 0209 and 0212 in the region traversed by the observed failure front. The configuration of experiment 0305 (Table I) was chosen such that location of the spall plane will be ahead of the region traversed by the failure front in SiC-B. In this experiment the spall plane was 5.05 mm from the impact surface of the target, while the failure front traveled, at the most, 4.45 mm into the target. Fig. 6 shows the free surface velocity profile recorded in this experiment. The value of spall strength of SiC-B obtained from this experiment is 0.39 ± 0.09 GPa and validates that the loss of spall strength observed in experiments 0209 and 0212 is due to the fact that spall plane was located in the region traversed by the failure front in SiC-B.

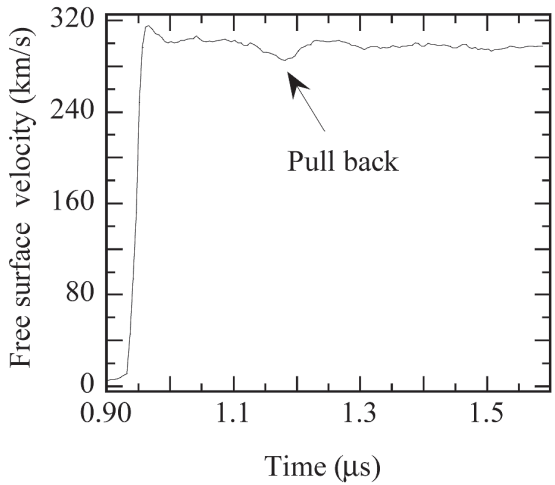

Fig. 6. Free surface velocity recorded in experiment 0305.

Discussion and Future Work

The results of spall experiments performed at 3.9 ± 0.1 GPa seem to be consistent with the hypothesis that the deformation of SiC-B to this stress is dominated by the effect of localized plastic deformation. Induced shear, under simultaneous compression shear, enhances this domination and permits SiC-B to retain and/or increase its spall strength. However, when shocked to 5.8 ± 0.1 GPa under induced shear, its deformation is also controlled by the observed propagation of failure front, which causes SiC-B to lose its spall strength in the region behind the front even as it continues to retain its spall strength in the region ahead of the front. The values of spall strength of SiC-B retained under normal impact and under simultaneous compression shear in experiments 0207 and 0305, i.e., 0.24 ± 0.06 and 0.39 ± 0.09 GPa, respectively, tend to suggest that (i) propagation of failure front in SiC-B is not manifested under normal impact at 5.8 ± 0.1 GPa, and (ii) under simultaneous compression shear the deformation ahead of the failure front appears to be controlled if not dominated by the plastic deformation as at 3.9 GPa. Thus the spallation of SiC-B, as demonstrated by the results of the experiments presented in this investigation, is much more complex than initially envisaged. Spallation in SiC-B is clearly dependent on the interplay of plastic deformation, very likely intra-granular in nature, micro/meso-crack generation and propagation at impurity and void sites, and failure front induced shear assisted dilation of a material as suggested by Grady.[9] The above suggested interplay is impossible to resolve with any confidence based on the present work, as a successful delineation of the suggested interplay to understand the spallation in SiC-B will in all probability require successful recovery of shocked SiC-B from a variety of shock loading conditions. Further, additional shock wave experiments which would assist in improving the current understanding of shock-induced response of SiC-B will require determination of: (i) impact stress and shear stress/strain thresholds needed to initiate the failure front in SiC-B, (ii) change in magnitudes of failure front velocity and of re-acceleration signal change with impact stress and shear stress/strain, (iii) the effect of failure front on compressibility and shear strength of the material in the region traversed by the front, and (iv) impact stress and shear stress/strain thresholds at which the failure front is coincident with the inelastic/shock wave propagation.

References

1. P. Bartkowski. and D. P. Dandekar, "Spall Strengths of Sintered and Hot-Pressed Silicon Carbide," *Shock Compression of Condensed Matter-1995*, eds. S. C. Schmidt and W. C. Tao, American Institute of Physics, New York, 535-539, 1996.
2. L. Ewart and D. P. Dandekar, "Relationship Between the Shock Response and Microstructural Features of Titanium Diboride (TiB_2)," *High-Pressure Science and Technology - 1993,* eds. S. C. Schmidt, J. W. Shaner, G. A. Samara, and M. Ross, American Institute of Physics, New York, 1201-1204, 1994.
3. D.P. Dandekar and P. T. Bartkowski, "Spall Strengths of Silicon Carbides Under Shock Loading," *Shock Wave and High-Strain rate Phenomena*, eds. K. P. Staudhammcr, L. E. Murr, and M. A. Meyers, Elsevier, New York, 71, 2001.
4. D.P. Dandekar, "Spall Strengths of Sintered and Hot-Pressed Silicon Carbide," Army Research Laboratory Technical Report, ARL-TR-2430, Army Research Laboratory, Aberdeen Proving Ground, MD, 2001.
5. L. M. Barker and R. E. Hollenbach, "Laser Interferometer for Measuring High Velocities of Any Reflecting Surface," *J. Appl. Phys.,* 43 4669-4680 (1972).

6. G. I. Kanel, S. V. Rasorenov, and V. E. Fortov, "The Failure Waves and Spallations in Homogeneous Brittle Materials," *Shock Compression of Condensed Matter-1991*, eds. S. C. Schmidt, R. D. Dick, J. W. Forbes, and D. G. Tasker, Elsevier, New York, 451-454, 1992.
7. D. P. Dandekar and P. A. Beaulieu, "Failure Wave Under Shock Compression in Soda Lime Glass," *Metallurgical and Material Applications of Shock-Wave and High Strain-Rate Phenomena*, eds. L. E. Murr, K. P. Satudhammer, and M. A. Meyers, Elsevier, Amsterdam, Netherlands, 211-218, 1995.
8. N. S. Brar and S. J. Bless, "Failure Waves in Glass Under Dynamic Compression," *High Press. Res.,* 10 773-784 (1992).
9. D. E. Grady, "Dynamic Properties of Ceramic Materials," Sandia National Laboratories Report, SAND 94-3266, Sandia National Laboratories, Albuquerque, NM, 1995.

NO. OF COPIES	ORGANIZATION
1 (PDF ONLY)	DEFENSE TECHNICAL INFORMATION CTR DTIC OCA 8725 JOHN J KINGMAN RD STE 0944 FT BELVOIR VA 22060-6218
1	COMMANDING GENERAL US ARMY MATERIEL CMD AMCRDA TF 5001 EISENHOWER AVE ALEXANDRIA VA 22333-0001
1	INST FOR ADVNCD TCHNLGY THE UNIV OF TEXAS AT AUSTIN 3925 W BRAKER LN STE 400 AUSTIN TX 78759-5316
1	US MILITARY ACADEMY MATH SCI CTR EXCELLENCE MADN MATH THAYER HALL WEST POINT NY 10996-1786
1	DIRECTOR US ARMY RESEARCH LAB IMNE AD IM DR 2800 POWDER MILL RD ADELPHI MD 20783-1197
3	DIRECTOR US ARMY RESEARCH LAB AMSRD ARL CI OK TL 2800 POWDER MILL RD ADELPHI MD 20783-1197
3	DIRECTOR US ARMY RESEARCH LAB AMSRD ARL CS IS T 2800 POWDER MILL RD ADELPHI MD 20783-1197

NO. OF COPIES	ORGANIZATION
	ABERDEEN PROVING GROUND
1	DIR USARL AMSRD ARL CI OK TP (BLDG 4600)

NO. OF COPIES	ORGANIZATION
1	CECOM SP & TRRSTRL COMMCTN DIV AMSEL RD ST MC M H SOICHER FT MONMOUTH NJ 07703-5203
1	PRIN DPTY FOR TCHNLGY HQ US ARMY MATCOM AMCDCGT R PRICE 5001 EISENHOWER AVE ALEXANDRIA VA 22333-0001
1	PRIN DPTY FOR ACQUSTN HQS US ARMY MATCOM AMCDCGA D ADAMS 5001 EISENHOWER AVE ALEXANDRIA VA 22333-00001
1	DPTY CG FOR RDE HQS US ARMY MATCOM AMCRD 5001 EISENHOWER AVE ALEXANDRIA VA 22333-00001
1	ASST DPTY CG FOR RDE HQS US ARMY MATCOM AMCRD COL S MANESS 5001 EISENHOWER AVE ALEXANDRIA VA 22333-00001
3	AIR FORCE ARMAMENT LAB AFATL DLJW W COOK D BELK J FOSTER EGLIN AFB FL 32542
1	DPTY ASSIST SCY FOR R & T SARD TT THE PENTAGON RM 3E479 WASHINGTON DC 20310-0103
1	DARPA L STOTTS 3701 N FAIRFAX DR ARLINGTON VA 22203-1714

NO. OF COPIES	ORGANIZATION
1	DIRECTOR US ARMY RESEARCH LAB AMSRL CS AL TA 2800 POWDER MILL ROAD ADELPHI MD 20783-1145
3	DIRECTOR US ARMY ARDEC AMSTA AR FSA E W P DUNN J PEARSON E BAKER PICATINNY ARSENAL NJ 07806-5000
2	US ARMY TARDEC AMSTRA TR R MS 263 K BISHNOI D TEMPLETON WARREN MI 48397-5000
4	COMMANDER US ARMY BELVOIR RD&E CTR STRBE N WESTLICH STRBE NAN S G BISHOP J WILLIAMS FORT BELVOIR VA 22060-5166
1	COMMANDER US ARMY RESEARCH OFFICE A RAJENDRAN PO BOX 12211 RESEARCH TRIANGLE PARK NC 27709-2211
1	NAVAL RESEARCH LAB A E WILLIAMS CODE 6684 4555 OVERLOOK AVE SW WASHINGTON DC 20375
6	DIRECTOR LANL P MAUDLIN R GRAY W R THISSELL A ZUREK Y HORIE F ADDESSIO PO BOX 1663 LOS ALAMOS NM 87545

NO. OF COPIES	ORGANIZATION
7	DIRECTOR SANDIA NATL LABS E S HERTEL JR MS 0819 W REINHART T VOLGER R BRANNON MS 0820 L CHHABILDAS MS 1811 M FURNISH MS 0821 M KIPP MS 0820 PO BOX 5800 ALBUQUERQUE NM 87185-0307
2	DIRECTOR LLNL J AKELLA N C HOLMES PO BOX 808 LIVERMORE CA 94550
2	CALTECH PROF G RAVICHANDRAN T J AHRENS MS 252 21 1201 E CALIFORNIA BLVD PASADENA CA 91125
2	ARMY HIGH PERFORMANCE COMPUTING RSRCH CTR T HOLMQUIST G JOHNSON 1200 WASHINGTON AVE S MINNEAPOLIS MN 55415
3	SOUTHWEST RESEARCH INSTITUTE C ANDERSON J WALKER K DANNEMANN PO DRAWER 28510 SAN ANTONIO TX 78284
2	UNIVERSITY OF DELAWARE DEPT OF MECH ENGINEERING PROF J GILLESPIE NEWARK DE 19716
3	SRI INTERNATIONAL D CURRAN D SHOCKEY R KLOPP 333 RAVENSWOOD AVE MENLO PARK CA 94025

NO. OF COPIES	ORGANIZATION
1	VIRGINIA POLYTECHNIC INST COLLEGE OF ENGINEERING R BATRA BLACKSBURG VA 24061-0219
1	COMPUTATIONAL MECHANICS CONSULTANTS J A ZUKAS PO BOX 11314 BALTIMORE MD 21239-0314
1	KAMAN SCIENCES CORP D L JONES 2560 HUNTINGTON AVE STE 200 ALEXANDRIA VA 22303
6	INST OF ADVANCED TECH UNIVERSITY OF TX AUSTIN S BLESS H FAIR D LITTLEFIELD C PERSAD P SULLIVAN S SATAPATHY 3925 W BRAKER LN STE 400 AUSTIN TX 78759-5316
1	APPLIED RSCH ASSOCIATES D E GRADY 4300 SAN MATEO BLVD NE STE A220 ALBUQUERQUE NM 87110
1	INTERNATIONAL RESEARCH ASSOCIATES INC D L ORPHAL 4450 BLACK AVE PLEASANTON CA 94566
1	THE DOW CHEMICAL CO CENTRAL RSRCH ENGINEERING LABORATORY M EL RAHEB BLDG 1776 MIDLAND MI 48640
1	BOB SKAGGS CONSULTANT S R SKAGGS 79 COUNTY RD 117 SOUTH SANTA FE NM 87501

NO. OF COPIES	ORGANIZATION
1	WASHINGTON ST UNIVERSITY SCHOOL OF MECHANCIAL AND MATERIAL ENGINEERING J L DING PULLMAN WA 99164-2920
2	WASHINGTON ST UNIVERSITY INSTITUTE OF SHOCK PHYSICS Y M GUPTA J ASAY PULLMAN WA 99164-2814
1	COORS CERAMIC COMPANY T RILEY 600 NINTH ST GOLDEN CO 80401
1	ARIZONA STATE UNIVERSITY MECHANICAL AND AEROSPACE ENGINEERING D KRAVCINOVIC TEMPE AZ 85287-6106
1	UNIVERSITY OF DAYTON RESEARCH INSTITUTE N S BRAR 300 COLLEGE PARK MS SPC 1911 DAYTON OH 45469
5	DIRECTOR USARL K WILSON FRENCH DEA 1396 ADELPHI MD 20783-1197

NO. OF COPIES	ORGANIZATION
	ABERDEEN PROVING GROUND
54	DIR USARL AMSRD WM E SCHMIDT T WRIGHT J MACAULEY AMSRD WM MB G GAZONAS J LASALVIA P PATEL AMSRL WM TA P BARTKOWSKI W A GOOCH M ZOLTOSKI E HORWATH M NORMANDIA AMSRL WM TC R COATES K KIMSEY D SCHEFFLER AMSRL WM TD S SEGELETES D DANDEKAR (30 CPS) K IYER M GREENFIELD J CLAYTON H W MEYER E RAPACKI S SCHOENFELD T BJERKE M SCHEIDLER T WEERASOORIYA

NO. OF COPIES	ORGANIZATION
1	DERA N J LYNCH WEAPONS SYSTEMS BLDG A20 DRA FORT HALSTEAD SEVENOAKS KENT TN 147BP UNITED KINGDOM
2	ERNST MACH INTITUT VOLKER HOHLER H NAHAME ECKERSTRASSE 4 D 7800 FREIBURG 1 BR 791 4 GERMANY
1	FOA2 P LUNDBERG S 14725 TUMBA SWEDEN
1	PCS GROUP CAVENDISH LABORATORY W G PROUD MADINGLEY RD CAMBRIDGE UNITED KINGDOM
1	CENTRE D ETUDES DE GRAMAT J Y TRANCHET 46500 GRAMAT FRANCE
1	MINISTERE DE LA DEFENSE DR G BRAULT DGA DSP STTC 4 RUE DE LA PORTE DISSY 75015 PARIS FRANCE
1	SPART DIRECTION BP 19 DR E WARINGHAM 10 PLACE GEORGES CLEMENCEOUX 92211 SAINT CLOUD CEDEX FRANCE

NO. OF COPIES	ORGANIZATION
1	ROYAL MILITARY COLLEGE OF SCIENCE CRANEFIELD UNIVERSITY PROF N BOURNE J MILLETT SHRIVENHAM SWINDON SN6 8LA UNITED KINGDOM
1	BEN GURIAN UNIVERSITY OF NEGEV E ZERETSKY DEPT OF MECH ENG BEER-SHEVA ISRAEL 84105
2	RUSSIAN ACADEMY OF SCIENCES INSTITUTE FOR HIGH ENERGY DENSITIES G I KANEL S V RAZORENOV IVTAN IZHORSKAYA 13/19 MOSCOW 127412 RUSSIA

INTENTIONALLY LEFT BLANK.